Biaxial Strain Measurements of J_C on a (RE)BCO Coated Conductor

Jack R. Greenwood, Elizabeth Surrey and Damian P. Hampshire

For several years it has been possible to measure the uniaxial strain dependence of the critical current density $J_C(\varepsilon)$ of (RE)BCO coated conductors ((RE)BCO tapes) and a parabolic strain dependence of $J_C(\varepsilon)$ has been observed. To improve our understanding of how strain affects the electrical and mechanical properties of a SuperPower APC SCS4050 (RE)BCO tape, we have created a biaxial sample holder which can apply arbitrary strains along both the *x*- and *y*-axes of a (RE)BCO tape simultaneously. It can be used to measure J_C for independently controllable applied *x* and *y* strains ranging from $-0.50\% \leq \varepsilon_x \leq 0.30\%$ and $-0.15\% \leq \varepsilon_y \leq 0.20\%$ respectively, at 77 K. We present the results of J_C measurements over this strain range at 77 K in magnetic fields of up to 0.7 T. We show that we obtain the standard parabolic relationship for $J_C(\varepsilon_x)$, with a peak in J_C occurring at $\varepsilon_{xP} = -0.01\%$. We also show that when we apply an additional *y* strain of $\varepsilon_y = -0.08\%$ the peak in J_C moves to $\varepsilon_{xP} = 0.4\%$, which cannot be explained by considering the differential strains produced by non-superconducting components of the tape and sample holder. In addition, the value of J_C at the peak increases considerably, by 11%.

***Index Terms*—Critical current, strain measurement, 2G HTS conductors, cuprates.**

I. Introduction

UNDERSTANDING the mechanisms responsible for the strain dependence of the critical current density (J_C) of 2nd generation, high temperature (RE)BCO coated conductors (often referred to as (RE)BCO tapes) allows tape manufacturers to optimize their fabrication processes and engineers to optimize systems in which the tapes are used. Over the last few years, experimental methods have been developed which allow these tapes to be strained uniaxially along the direction of current flow, so J_C can be measured as a function of applied uniaxial strain (ε). One of the most popular methods is to use a bending beam apparatus, as it allows both compressive and tensile strains to be applied to a tape [1, 2].

It is well established that there is a parabolic relationship between J_C and applied uniaxial strain [3, 4]. The peak in J_C may occur at either a tensile or compressive strain [5]. Differential thermal contraction between the component parts of the (RE)BCO tape (as well as the sample holder) can cause the (RE)BCO layer to have a non-zero strain even when no external strain has been applied. The complex microtwinned structure of the (RE)BCO layer in a tape also affects its mechanical and superconducting properties [5, 6]. In this paper we have measured SuperPower APC SCS4050 (RE)BCO tapes. The superconducting layer consists of a series of A or B domains which have their *a*- or *b*-axes aligned with the direction of current flow respectively. Single crystal measurements have shown that the strain dependence of the critical temperature (T_C) along the *a*-axis is opposite to that along the *b*-axes [7]. From these measurements, a 1-dimensional chain model has been proposed which explains the location of the peak in J_C by considering the total fractions of A and B domains in the (RE)BCO layer and the strain dependence of T_C in single crystals [8]

To improve our understanding of how the microtwinned structure of the (RE)BCO layer affects the strain dependence of J_C, and to optimise the use of tapes in applications such as CORC® cables where tapes are in complex strain states [9, 10], we have designed and commissioned a new biaxial sample holder known as the 'crossboard'. This sample holder can be used to investigate the strain dependence of J_C for arbitrarily chosen *x* and *y* strains. The key features of the crossboard and the experimental procedure for performing biaxial strain dependent J_C measurements are outlined in Section II. Section III presents results for the temperature dependence of the applied strains, as the strains are applied at room temperature, but J_C measurements are made at 77 K. Section III also presents results for the biaxial strain dependence of J_C at 77 K, for magnetic fields up to 0.7 T. The biaxial strain dependent J_C data are discussed in further detail in Section IV and the capabilities of the crossboard are also discussed. Some conclusions are presented in Section V.

II. Sample Holder & Experimental Method

A. Sample Holder Geometry & Assembly

The geometry of the crossboard is shown in Fig. 1. The crossboard is manufactured from Berylco® 25. Stainless steel grippers constrain the crossboard in the *z* direction and prevent *z*

Manuscript receipt and acceptance dates will be inserted here. This work was funded by EPSRC grant EP/L01663X/1 for the Fusion Doctoral Training Network. This work has been carried out within the framework of the EUROfusion Consortium and has received funding from the Euratom research training program 2014-2018 under grant No. 633053. The data are available at http://dx.doi.org/10.15128/r1jm214p120 and associated materials are on the Durham Research Online website: http://dro.dur.ac.uk .

J. R. Greenwood and D. P. Hampshire are with Durham University, Department of Physics, Superconductivity Group, Durham DH1 3LE, UK (e-mail: jack.r.greenwood@durham.ac.uk; d.p.hampshire@durham.ac.uk).

E. Surrey is with the European Atomic Energy Community (EURATOM)/ Culham Center for Fusion Energy (CCFE) Fusion Association, Culham Science Center, Abingdon OX14 3DB, U.K.

Color versions of one or more of the figures in this paper are available online at http://ieeexplore.ieee.org.

Digital Object Identifier will be inserted here upon acceptance.

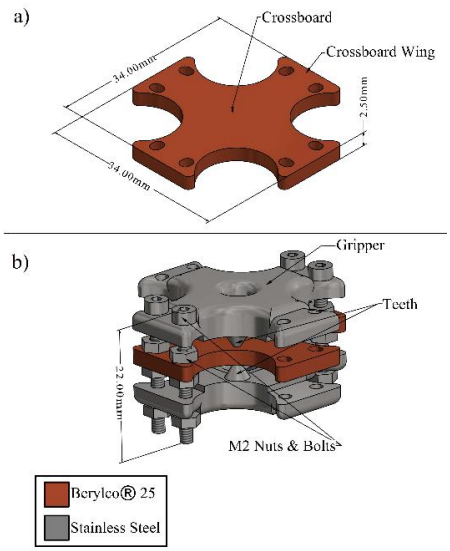

Fig. 1. (a) A CAD model of the crossboard. (b) A CAD model of the assembly used to apply x or y strains on the top side of the crossboard. The combination of nuts and bolts shown allows strains to be applied in the y direction.

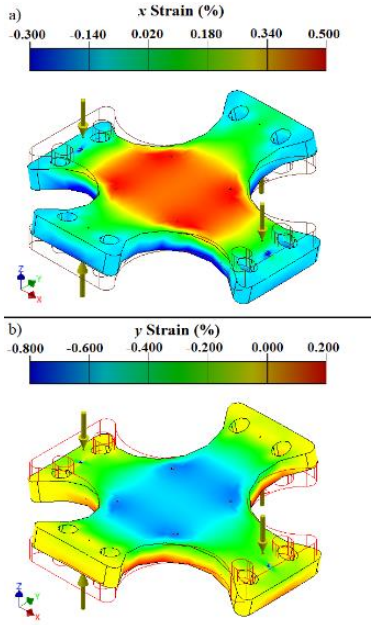

Fig. 2. (a) The x strain distribution on the surface of the crossboard when an 1800 N force is applied at the positions of the arrows at room temperature. (b) The corresponding y strain distribution.

strains from being generated at the center of the crossboard. Tightening the nuts and bolts cause the wings of the crossboard to bend around the teeth of the steel grippers, which generates x or y strains at the center of the crossboard. Both tensile and compressive strains can be independently generated in each direction – hence any combination of x and y strain within the strain limits of the crossboard can be applied to a tape.

B. *Strain Homogeneity*

Finite element simulations have been performed on the crossboard to evaluate its strain homogeneity. The results of one simulation are depicted in Fig. 2. In this simulation, 4 loads of 1800 N each are applied at the positions of the arrows. The x and y strains at the center of the crossboard are $\varepsilon_{xC} = 0.48\%$ and $\varepsilon_{yC} = -0.48\%$ respectively. The variations in x and y strain in the central 7 mm of the crossboard along its x-axis are $\Delta\varepsilon_{xC} = 0.025\%$ and $\Delta\varepsilon_{yC} = 0.002\%$ respectively. In another simulation, strain was applied along just one axis and the value of $\partial\varepsilon_y/\partial\varepsilon_x$ at the center of the crossboard was -0.42.

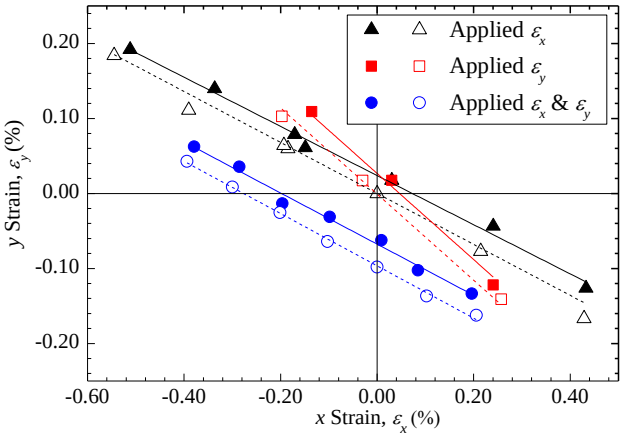

Fig. 3. The effect of temperature on the applied strains ε_x and ε_y as measured by the strain gauge. The dashed linear fits and open data points are for strains applied at room temperature. The solid linear fits and closed data points are for the strains at 77 K.

TABLE I
FREE-PARAMETER VALUES FROM THE LINEAR FITS IN FIG. 3.

Applied Strain Type	Temperature (K)	$\frac{\partial\varepsilon_y}{\partial\varepsilon_x}$	$\varepsilon_y(\varepsilon_x = 0)$ (%)
Applied ε_x ●	300	−0.34	0
	77	−0.33	0.024
Applied ε_y ●	300	−0.574	0
	77	−0.574	0.027
Applied ε_x & ε_y ●	300	−0.349	−0.097
	77	−0.34	−0.068

C. *Experimental Method*

$J_C(B, \theta, \varepsilon_x, \varepsilon_y)$ d.c. current transport measurements have been performed on tapes at 77 K, using the crossboard sample holder and the standard four-terminal technique. A tape with a length of 24 mm and a width of 4 mm was soldered with its substrate side facing downwards onto the center of the crossboard using 60/40 Sn/Pb solder. The tape was aligned so the direction of current flow was along the x-axis of the crossboard. Current leads were attached to the ends of the tape and two pairs of voltage taps were attached about the center of the tape with separations of ~ 7.0 mm and ~ 10.0 mm. A HBM XY91-1.5/120 T rosette strain gauge containing two sensors was attached to the center of the tape, such that strain could be measured parallel and orthogonal to the current flow [11]. The sensitive area of the strain gauge is ~ 1 mm^2.

The crossboard and grippers are attached to a probe which can be placed in an open liquid nitrogen Dewar. At room temperature, the nuts and bolts are adjusted to set the strain. The crossboard is then cooled to 77 K and the strain re-measured.

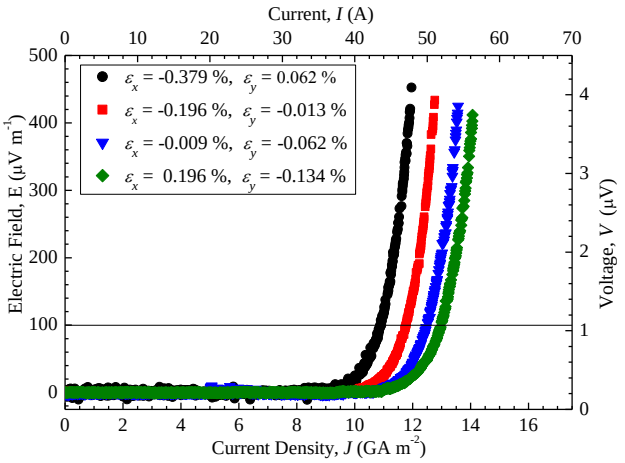

Fig. 4. *E-J* plots for four different values of ε_x and ε_y at 77 K. The magnetic field was 0.2 T and was applied parallel to the *z*-axis of the crossboard.

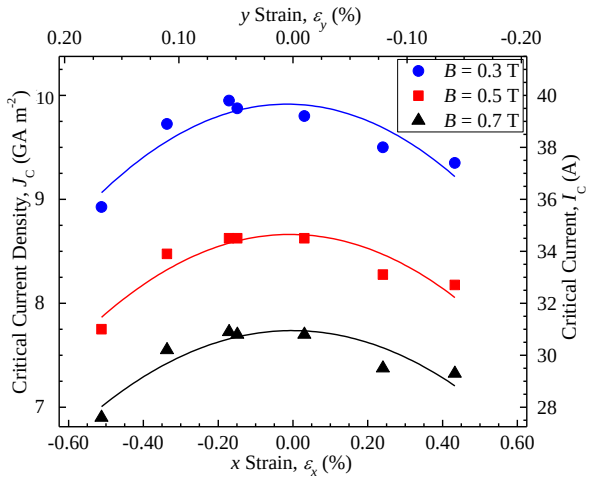

Fig. 5. The strain dependence of J_C at 77 K as a function of strain. ε_x was the independent variable. ε_y is calculated from the corresponding linear fit in Fig. 3. The magnetic field was applied parallel to the *z*-axis of the crossboard.

The probe is connected to a 120 A power supply. A 0.7 T horizontal magnet system is used to apply a magnetic field to the tape. The magnet system can be rotated 360° around the *x*-axis of the crossboard, allowing variable field and variable angle measurements to be made.

III. Results

A. Temperature Dependence of Strain Coordinates

Three different combinations of strain have been applied to the (RE)BCO tape and are reported here. Strains have been applied along the *x* direction only, the *y* direction only and along both the *x* and *y* directions. Fig. 3 shows the effect of temperature on the applied strains and Table I lists the values of the linear fits shown in Fig. 3. The change in temperature changes the values of $\varepsilon_y(\varepsilon_x = 0)$ by ~ 0.03% but doesn't change the gradients very significantly, and the values of *x* and *y* strain at 77 K are reasonably reproducible. When both *x* and *y* strains were applied to the tape simultaneously (blue data), the tape was strained to specific strain states so that a linear fit of the strain coordinates to be generated, with a value of $\partial\varepsilon_y/\partial\varepsilon_x$ of ~0.34 to

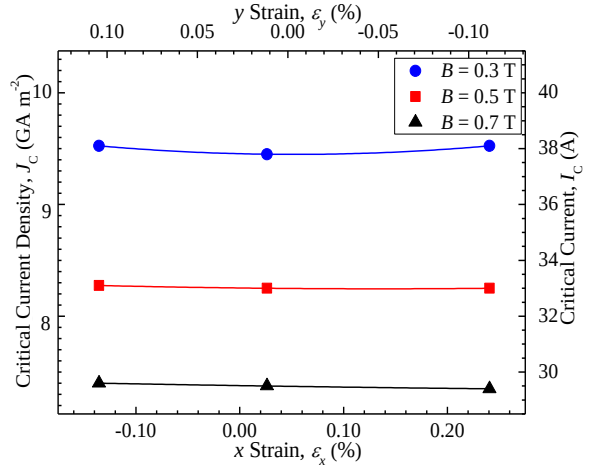

Fig. 6. The strain dependence of J_C at 77 K as a function of strain. ε_y was the independent variable. ε_x is calculated using the corresponding linear fit in Fig. 3. The magnetic field was applied parallel to the *z*-axis of the crossboard.

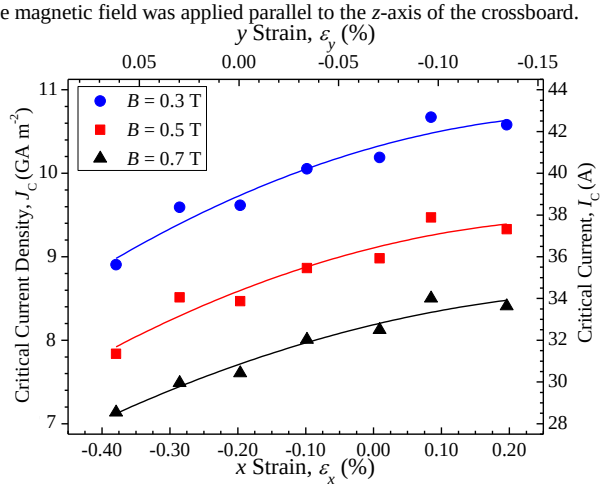

Fig. 7. The strain dependence of J_C at 77 K as a function of strain. ε_y was first set to a compressive strain of ~ −0.08% and then ε_x was used as the independent variable. ε_y is calculated using the corresponding linear fit in Fig. 3. The magnetic field was applied parallel to the *z*-axis of the crossboard.

match the applied *x* strain (black) data. The values of $\partial\varepsilon_y/\partial\varepsilon_x$ will be discussed in greater detail in the Section IV.

B. E - J Characteristics

In this paper, to calculate the values of *J* and J_C, we have assumed the (RE)BCO layer has a thickness of 1.0 μm. Fig. 4 shows *E* - *J* plots for different values of *x* and *y* strain. The strains correspond to a subset of the applied ε_x and ε_y (blue) strain coordinates in Fig. 3. J_C is determined at $E = 100\ \mu V\ m^{-1}$. The values of J_C increase monotonically with increasing tension along the *x*-axis. There is no sign of a peak in J_C over the range of *x* and *y* strains measured.

C. Biaxial Strain Dependence of J_C

The parabolic fits shown in Fig. 5, Fig. 6 and Fig. 7 for $J_C(\varepsilon_x)$ are fitted using the equation

$$\frac{J_C(\varepsilon_x)}{J_C(\varepsilon_x = 0)} = 1 - \beta(\varepsilon_x - \varepsilon_{xP})^2 + \beta\varepsilon_{xP}^2, \quad (1)$$

TABLE II
VALUES FOR THE PARABOLIC FITS IN FIG. 5, FIG. 6 & FIG. 7 .

Applied Strain Type	ε_{xP} (%)	ε_{yP} (%)	β (%$^{-2}$)	$J_C(\varepsilon_x = \varepsilon_{xP})$ (GA m^{-2})
Applied ε_x	−0.01	0.03	0.38	8.65
Applied ε_y	0.1	0	0	8.3
Applied ε_x & ε_y	0.4	-0.2	0.3	9.61

The values presented are for the B = 0.5 T data, with the magnetic field applied perpendicular to the z-axis of the crossboard.

where $J_C(\varepsilon_x = 0)$ is the critical current density at zero x strain, β is a fitting constant and ε_{xP} is the applied x strain at which J_C reaches its highest value [4, 5]. Two neighbouring pieces of tape from the same spool were used to collect the $J_C(B, \varepsilon_x, \varepsilon_y)$ data. Fig. 5 and Fig. 6 show data for one piece of tape and Fig. 7 shows data for the other. At zero strain, the self-field values of J_C for the two tapes were 22.2 GA m^{-2} and 23.4 GA m^{-2} (~5% different). This difference increased to 7 % at 0.5 T. To account for these differences, the J_C data plotted in Fig. 7 for the second tape have been renormalized using the $J_C(B, \varepsilon_x, \varepsilon_y)$ data of the first tape at zero strain.

Fig. 5 shows the strain dependence of J_C at 77 K when x strains are applied to the tape. The standard parabolic relationship between J_C and ε_x is observed and the peak in J_C occurs at $\varepsilon_{xP} = -0.01\%$. Fig. 6 shows the strain dependence of J_C when y strains are applied to the tape. There is no clear peak in J_C across the strain range of $-0.1\% \leq \varepsilon_y \leq 0.2\%$. Fig. 7 shows the strain dependence of J_C at 77 K when both x and y strains are applied to the tape. There is still a parabolic relationship between J_C and ε_x, but the strain at which the peak in J_C occurs has changed, to a tensile strain of $\varepsilon_{xP} = 0.4\%$ and the peak value of J_C has increased from 8.65 GA m^{-2} to 9.61 GA m^{-2}. Table II summarises the parameters obtained at 0.5 T from the parabolic fits to the above equation using the data in Fig. 5 to Fig. 7.

IV. DISCUSSION

The value of $\partial\varepsilon_y/\partial\varepsilon_x$ shown in Fig. 3 when strain is applied along the x-axis is −0.34, whereas when the strain is applied along the y-axis it is considerably lower (-0.574). To investigate this difference, we have completed measurements of $\partial\varepsilon_y/\partial\varepsilon_x$ on a 4 mm × 4 mm piece of tape and found value of −0.48 for applied x strains and −1/0.48 for applied y strains as expected. Hence we conclude that the tape affects the mechanical behavior of the crossboard and attribute the −0.574 value observed for the long tape to the asymmetric nature of the crossboard/tape system. We attribute the change in values of strain when the crossboard is cooled from room temperature to 77 K, to the differential thermal contraction between the components of the crossboard assembly.

With regards to the biaxial strain dependence of J_C, the large change in ε_{xp}, which occurs when an additional compressive y strain of $\varepsilon_y \sim -0.08\%$ is applied (c.f. Fig. 5 and Fig. 7), cannot be explained by considering the strains produced by other components of the tape and sample holder. The data in Fig. 6 is limited. More data is required to determine the strain value at which $J_C(\varepsilon_x)$ reaches its peak value. A 1-dimensional chain model [5, 8] has been developed to explain the uniaxial strain dependence of J_C in tapes with no artificial pinning centres (APCs). This model could be extended to two dimensions if the biaxial strain dependence of T_C in single crystals of (RE)BCO was known. The tapes measured for this paper contained APCs, which may influence the behaviour of $J_C(B, \varepsilon_x, \varepsilon_y)$.

Further improvements could be made to the crossboard to improve its strain range and shorten the time taken to perform measurements. The main limitation of the crossboard is that the strains must be applied at room temperature. Although we have shown that we can predict the strain state of the (RE)BCO tape at 77 K from the tape's strain state at room temperature, it would be advantageous to change strains while remaining at 77 K. Of course ideally we would like to be able to change strain in all three directions independently.

V. CONCLUSION

We have designed and commissioned a new biaxial sample holder, known as the 'crossboard', which can be used to measure J_C for arbitrarily chosen strains along the x- and y-axes of a (RE)BCO coated conductor in the ranges of $-0.50\% < \varepsilon_x < 0.30\%$ and $-0.15\% < \varepsilon_y < 0.20\%$, at 77 K. J_C measurements have been made at 77 K in fields up to B = 0.7 T and the standard parabolic relationship between applied x strains and J_C has been observed. We have shown that by applying an additional compressive y strain of −0.08% at 77 K, the peak in $J_C(\varepsilon_x)$ moves from a compressive x strain of $\varepsilon_x = -0.01\%$ to a tensile strain of 0.4%. The value of J_C at the peak also increases considerably, by 11%. The movement of the strain peak position cannot be explained by considering the strains exerted on the (RE)BCO layer from the other materials in the tape or sample holder alone. Having the ability to apply biaxial strains to a (RE)BCO coated conductor opens exciting new possibilities to study both the mechanical and electrical properties of these tapes in two dimensions.

ACKNOWLEDGMENT

The authors would like to thank Professor K. Osamura, R. Davey and S. Wilkins for many useful discussions. We also thank Steve Lishman in the Durham Mechanical Workshop for helping to develop the design of the crossboard.

REFERENCES

[1] P. Sunwong, J. S. Higgins, and D. P. Hampshire, "Probes for investigating the effect of magnetic field, field orientation, temperature and strain on the critical current density of anisotropic high-temperature superconducting tapes in a split-pair 15 T horizontal magnet,", *The Review of Scientific Instruments*, vol. 85, no. 6, p. 065111, 2014.

[2] D. C. van der Laan and J. W. Ekin, "Dependence of the critical current of YBaCuO coated conductors on in-plane bending," *Supercond. Sci. and Technol.*, vol. 21, 2008.

[3] P. Sunwong, J. S. Higgins, Y. Tsui, M. J. Raine, and D. P. Hampshire, "The critical current density of grain boundary channels in polycrystalline HTS and LTS superconductors in magnetic fields," *Superconductivity Science and Technology*, vol. 26, p. 095006, 2013.

[4] J. S. Higgins and D. P. Hampshire, "Critical Current Density of $YBa_2Cu_3O_{7-\delta}$ Coated Conductors Under High Compression in High Fields," *IEEE Transactions on Applied Superconductivity*, vol. 21, no. 3, pp. 3234-3237, 2011.

[5] K. Osamura, S. Machiya, and D. P. Hampshire, "Mechanism for the uniaxial strain dependence of the critical current in practical REBCO tapes," *Superconductor Science & Technology*, vol. 29, no. 6, Jun 2016, Art. no. 065019.

[6] K. Osamura *et al.*, "Microtwin Structure and Its Influence on the Mechanical Properties of REBCO Coated Conductors," *IEEE Transactions on Applied Superconductivity*, vol. 22, no. 1, pp. 8400809-8400809, 2012.

[7] W. H. Fietz, K. P. Weiss, and S. I. Schlachter, "Influence of intrinsic strain on T-c and critical current of high-T-c superconductors," (in English), *Superconductor Science & Technology*, Article; Proceedings Paper vol. 18, no. 12, pp. S332-S337, Dec 2005.

[8] P. Branch, Y. Tsui, K. Osamura, and D. P. Hampshire, "Multimodal strain dependence of the critical parameters in high-field technological superconductors " *Submitted to Super. Sci and Tech.*, 2017.

[9] D. C. van der Laan, X. F. Lu, and L. F. Goodrich, "Compact GdBa2Cu3O7-delta coated conductor cables for electric power transmission and magnet applications," *Superconductor Science & Technology*, vol. 24, no. 4, Apr 2011, Art. no. 042001.

[10] J. D. Weiss, T. Mulder, H. J. ten Kate, and D. C. Van der Laan, "Introduction of CORC® wires: highly flexible, round high-temperature superconducting wires for magnet and power transmission applications," *Superconductor Science and Technology*, vol. 30, 2017.

[11] *Y series strain gages*. Available: www.nvms.com.au/wp-content/uploads/2014/07/Y-Series-Product-Catalogue.pdf. Accessed: 13 September 2017